

# Momentum Transport and Stable Modes in Kelvin-Helmholtz Turbulence

A.E. Fraser,<sup>1</sup> P.W. Terry,<sup>1</sup> and E.G. Zweibel<sup>1</sup>

*University of Wisconsin - Madison*

The Kelvin-Helmholtz (KH) instability, which arises in astrophysical and fusion systems with inhomogeneous flows, has an unstable and a stable mode at the same scales. We show that in KH turbulence, as in other types of turbulence, the stable mode is nonlinearly excited, affecting transport and nonlinearly removing energy from the inertial-range cascade to small scales. We quantify energy transfer to stable modes and its associated impact on turbulent amplitudes and transport, demonstrating that stable modes regulate transfer in KH systems. Finally, a quasilinear momentum transport calculation is performed to quantify the reduction in momentum transport due to stable modes.

## I. INTRODUCTION

Sheared flows are encountered in a variety of different systems. In the atmosphere, shear-flow instabilities are observed in cloud patterns<sup>1</sup>. In fusion devices, turbulence generates sheared zonal flows that are potentially unstable<sup>2</sup>. Shear-flow instabilities are especially important in astrophysics, where differential velocities are produced by a host of processes in a variety of settings, including jets driven by accretion of mass onto compact objects such as protostars or supermassive black holes, intergalactic clouds falling into a galaxy, and galaxies plowing through the intracluster medium. In astrophysical systems, it is thought that shear-flow instabilities induce formation of a turbulent shear layer, resulting in entrainment of material through turbulent momentum transport<sup>3</sup>, thermal and chemical mixing<sup>4</sup>, and possibly acceleration of particles to high energy<sup>5</sup>.

The number of potential applications makes quantitative models of turbulence driven by sheared flows highly desirable. Analytical models that describe spectral properties are important because both the separation between scales and Reynolds numbers found in astrophysical systems are much larger than what can typically be obtained in converged simulations<sup>11,12</sup>.

Many of these models, such as quasilinear transport calculations, assume the turbulence is driven by a shear-flow instability, and calculate transport based on the growth rate and mode structure of the linearly unstable eigenmodes of the system. These models are advantageous because they rely on the well-understood linear properties of various shear-flow instabilities<sup>6</sup>. Unfortunately, less is understood about the properties of these systems as they move into the turbulent regime where dynamics are highly nonlinear. It is often assumed that energy cascades through an inertial range to smaller, dissipative scales, much like forced Navier-Stokes turbulence. Additionally, though the systems admit eigenmodes that are stable, they are neglected.

In studies of instability-driven turbulence in gyroradius-scale systems relevant to fusion devices, the role that previously-neglected, large-scale structures play in instability saturation and turbulent diffusivities has been investigated for over a decade<sup>7</sup>. The structures are eigenmodes of the linearized system, are often at the same length scale as the driving instability, and have

been referred to as stable modes if their growth rates are negative<sup>8</sup>, or as subdominant modes if their growth rate is positive but smaller than that of the most unstable mode<sup>14</sup>. When perturbations are small and only the linear dynamics are considered, these modes are negligible compared to the most unstable mode. However, as the most unstable mode grows in amplitude, the nonlinear interactions between it and the stable modes can pump energy into the stable modes, causing them to grow and have a significant impact on the turbulence. In collisionless trapped electron mode turbulence, stable modes radically change the dynamics of the system, including changing the direction of particle flux<sup>8,13</sup>. In recent studies of plasma microturbulence in stellarators, quasilinear calculations of energy transport cannot reproduce the results of nonlinear simulations without including every subdominant unstable mode<sup>14</sup>.

While it has been demonstrated in the context of gyroradius-scale instabilities and turbulence in fusion plasmas that stable modes are universally excited and can have significant impacts on turbulence, their effects have not been studied in global-scale hydrodynamic or MHD instabilities. This paper presents a hydrodynamic system with global-scale eigenmodes where we demonstrate the nonlinear excitation of stable modes and quantify their impact on the turbulence using techniques that were successful in plasma microturbulence. We extend the tools developed in previous analytic calculations, where the systems were quasihomogeneous, to analyze nonlinear excitation in the inhomogeneous environment of unstable shear flows.

The paper is organized as follows. In Sec. II we present an unstable shear flow and discuss its unstable and stable eigenmodes. In Sec. III we develop a mapping of the total flow into the eigenmodes that allows a quantitative description of the energy transfer between the unstable and stable modes. In Sec. IV we use the tools of previous calculations to assess the level to which stable modes are excited relative to unstable modes in saturation. In Sec. V we consider the impact of stable modes on turbulent momentum transport. Conclusions are presented in Sec. VI.

## II. LINEAR MODES

We are investigating a piecewise linear equilibrium flow in the  $x$  direction with variation in the  $z$  direction, often referred to as the shear layer.  $\mathbf{v}_0 = (U(z), 0, 0)$ , where

$$U(z) = \begin{cases} U_0 & z \geq d \\ z \frac{U_0}{d} & -d \leq z \leq d \\ -U_0 & z \leq -d. \end{cases}$$

The shear layer provides the simplest shear flow instability for which the nonlinear driving of stable modes can be analyzed. The vortex sheet<sup>6</sup> is an even simpler manifestation of shear flow instability, but the discontinuous equilibrium flow leads to a discontinuous eigenmode structure. The eigenmode projection of the nonlinearity, calculated in the following section, involves a product of derivatives of the eigenmodes (see Eq. (9)), and such a product is not well-defined for discontinuous eigenmodes. Here, flow is assumed to be 2D ( $\partial/\partial y = 0$ ), inviscid, and incompressible. It has been shown that for unmagnetized shear flows, 2D perturbations are the most unstable<sup>6</sup>, so it suffices to restrict this analysis to the 2D system. The inviscid assumption simplifies the calculation, although in physical systems at scales much smaller than those considered here, viscosity acts to remove energy from perturbations. The assumption of incompressibility is convenient because of the stabilizing effect of compressibility in shear flow instabilities. This allows the perturbed velocity to be written in terms of a stream function  $\mathbf{v}_1 = \hat{y} \times \nabla \Phi(x, z) = (D\Phi, 0, -\partial\Phi/\partial x)$  where  $D \equiv d/dz$ . The perturbed vorticity is then entirely in the  $-\hat{y}$  direction and is governed by the vorticity equation,

$$\frac{\partial}{\partial t} \nabla^2 \Phi + U \frac{\partial}{\partial x} \nabla^2 \Phi - \frac{\partial \Phi}{\partial x} D^2 U + D\Phi \frac{\partial}{\partial x} \nabla^2 \Phi - \frac{\partial \Phi}{\partial x} D \nabla^2 \Phi = 0. \quad (1)$$

We drop terms nonlinear in  $\Phi$  and investigate normal modes of the form  $\Phi(x, z, t) = \phi(k, z) e^{i\omega(k)t} e^{ikx}$ . If we find that  $\text{Im}(\omega(k)) < 0$  for some mode at wavenumber  $k$ , then the mode will grow exponentially in time and is unstable. If  $\text{Im}(\omega(k)) > 0$ , the mode decays and is stable. If  $\text{Im}(\omega(k)) = 0$ , the mode is marginally stable. We take Fourier modes in  $x$  because Eq. (1) is homogeneous in  $x$ , but the dependence of  $U$  on  $z$  implies that Fourier modes in  $z$  are not solutions to the linear equation. This significantly complicates the analysis of stable mode interactions, as discussed in the following section.

The linearized equation for the normal modes is

$$(\omega + kU)(D^2 - k^2)\phi - k\phi D^2 U = 0. \quad (2)$$

Solutions of this system are well known<sup>6</sup>, but usually only the growth rate of the unstable mode or its eigenfunction is sought. We reexamine the problem to keep track of both the unstable and stable modes, in order to investigate their interaction through the nonlinearities in Eq. (1).

Note that for the shear layer,  $D^2 U$  is singular at  $z = \pm d$ . For  $|z| \neq d$  however,  $D^2 U = 0$ , so

$$(\omega + kU)(D^2 - k^2)\phi = 0$$

(for  $|z| \neq d$ ).

Solutions are given by either  $\omega + kU = 0$  or  $(D^2 - k^2)\phi = 0$ . While modes that satisfy the former are solutions of the system (for instance, modes that oscillate with  $\omega = -kU$  above and below the layer but satisfy  $(D^2 - k^2)\phi = 0$  within the layer), we are interested in stable and unstable modes, which requires  $\text{Im}(\omega) \neq 0$ . Therefore we construct eigenmodes from  $(D^2 - k^2)\phi = 0$ . It has been shown that for shear flow instabilities, the initial value calculation admits additional modes that decay algebraically<sup>15</sup>. While these modes potentially play a role in saturation of the instability and should be considered eventually, it makes sense to focus first on the interaction between the exponentially growing and decaying modes. Both the exponentially and algebraically decaying modes are ignored in quasilinear models of turbulence, so for the purposes of this paper it suffices to demonstrate the importance of just one of them. Focusing on solutions of  $(D^2 - k^2)\phi = 0$ , modes are then given by

$$\phi(z) = \begin{cases} ae^{-|k|z} & z > d \\ e^{|k|z} + be^{-|k|z} & -d < z < d \\ ce^{|k|z} & z < -d, \end{cases} \quad (3)$$

with constants  $a, b, c$  to be determined.

$U(z)$  is continuous at the boundaries of the shear layer, which we assume to be fixed at  $z = \pm d$ , therefore  $\phi$  must be as well<sup>6</sup>, so  $a$  and  $c$  can each be written in terms of  $b$ . Though  $U(z)$  and  $\phi$  are continuous at  $z = \pm d$ , the discontinuities in  $DU(z)$  lead to discontinuities in  $D\phi$ . The jump conditions that determine these discontinuities are obtained by integrating Eq. (2) from  $-d - \epsilon$  to  $-d + \epsilon$  and from  $d - \epsilon$  to  $d + \epsilon$ , then taking  $\epsilon \rightarrow 0$ :

$$\lim_{\epsilon \rightarrow 0} (\omega \pm kU_0) D\phi|_{\pm d \pm \epsilon} \pm k\phi(\pm d) \frac{U_0}{d} = 0 \quad (4)$$

After inserting Eq. (3), these form two constraints on  $b$  in terms of  $\omega(k)$  that can be solved to obtain the dispersion relation,

$$\omega = \pm \frac{e^{-2|k|d} U_0}{2d} \sqrt{e^{4|k|d} (1 - 2|k|d)^2 - 1}. \quad (5)$$

Fig. 1 shows how the growth rates and frequencies depend on wavenumber. Note that  $\omega^2 < 0$  for  $0 < |k|d \lesssim 0.64$ . For  $\omega^2 > 0$ , we shall refer to the negative and positive choices of  $\omega$  as  $\omega_1$  and  $\omega_2$ , respectively. For  $\omega^2 < 0$ , we choose  $\omega_1$  to be the unstable root, and  $\omega_2$  the stable one. Because  $b$  depends on  $\omega$  through Eq. (4) and the eigenmode structure  $\phi(z)$  depends on  $b$  through Eq. (3), the two solutions for  $\omega$  correspond to two different eigenmodes  $\phi(z)$ . We identify  $b_j$  and  $\phi_j$  as the  $b$  and

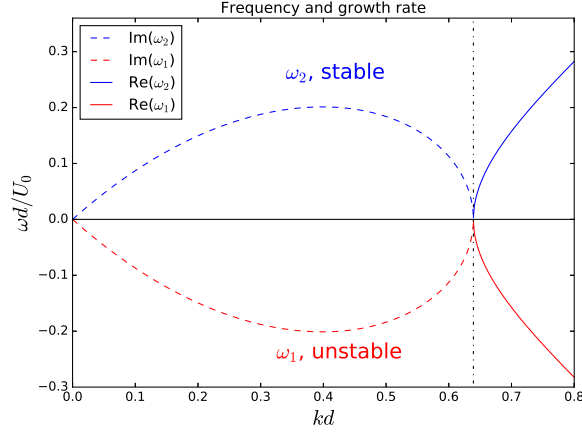


FIG. 1. Growth rate ( $\text{Im}(\omega)$ ) and frequency ( $\text{Re}(\omega)$ ) of the two modes. For  $|k|d \lesssim 0.64$  one mode is unstable and the other is stable, while for  $|k|d \gtrsim 0.64$  both modes are marginally stable.

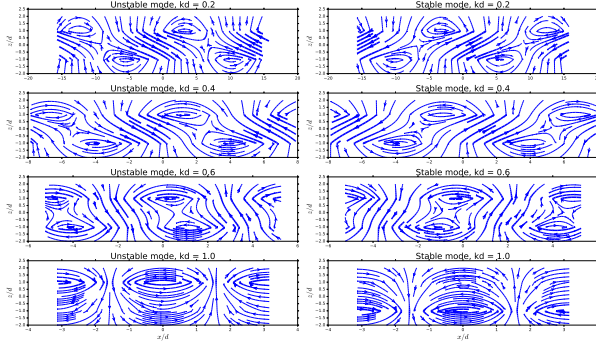


FIG. 2. Velocity profiles of  $\phi_1$  (left column) and  $\phi_2$  (right column) at various wavenumbers plotted over one wavelength in  $x$  and from  $z = -2d$  to  $z = 2d$ . Streamlines are plotted with line thickness proportional to flow speed. Each row corresponds to a different wavenumber  $k$ . The first three rows are in the unstable range, where  $\phi_1$  grows exponentially while  $\phi_2$  decays exponentially. The last row is a marginally stable wavenumber, where both  $\phi_1$  and  $\phi_2$  oscillate without any growth.

$\phi$  corresponding to  $\omega_j$ . The eigenmodes are then

$$\phi_j(k, z) = \begin{cases} (e^{2|k|d} + b_j)e^{-|k|z} & z > d \\ e^{|k|z} + b_j e^{-|k|z} & -d < z < d \\ (1 + b_j e^{2|k|d})e^{|k|z} & z < -d, \end{cases} \quad (6)$$

where

$$b_j = e^{2|k|d} \frac{2|k|d(\omega_j + kU_0) - kU_0}{kU_0}$$

satisfies  $b_1(k) = 1/b_1(-k) = b_2(-k) = 1/b_2(k)$  for all  $k$ , and also satisfies  $|b_j| = 1$  and  $b_1 = b_2^*$  for  $\omega^2 < 0$ . For  $\omega^2 < 0$ , the eigenmodes are nearly identical but satisfy  $\phi_1(k, z) = \phi_2^*(k, z)$ . Figure 2 shows the flows corresponding to these eigenmodes, and Fig. 3 shows what various

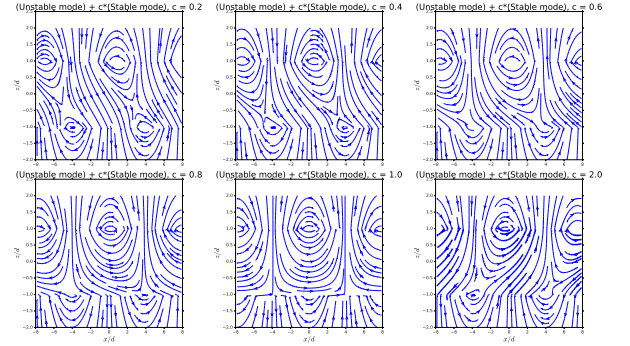


FIG. 3. Velocity profiles of combinations of both modes at  $kd = 0.4$  plotted over one wavelength in  $x$  and from  $z = -2d$  to  $z = 2d$ . In each successive panel the stable mode has a larger contribution to the overall flow. In this figure, the stable and unstable modes have the same phase. Changing the relative phase between the modes does impact the velocity profile, but the general trends remain unchanged.

linear combinations of stable and unstable modes look like. Figure 3 shows that an excitation of stable modes corresponds to a significant change in structure of the flow. Since nonlinear simulations of sheared flows show that they often give rise to secondary instabilities<sup>11</sup>, this suggests that the growth rates of these secondary instabilities depend significantly on the amplitude of stable modes of the primary instability in a turbulent state.

In standard descriptions of turbulence and quasilinear transport calculations it is common practice to neglect stable modes. This is typically justified by their linear exponential decay from an infinitesimal initial value. In this calculation we will account for the nonlinear drive of the stable mode by the unstable mode and investigate its impact on the evolution of the system.

### III. EIGENMODE PROJECTION

In the previous calculations of stable mode excitation<sup>8,10</sup>, arbitrary perturbations of dynamical quantities such as flow and pressure about an unstable equilibrium were expanded as linear combinations of the eigenmodes. Because the systems were homogeneous, the dynamical quantities of interest were the Fourier transforms of flows and pressures, and the governing systems of PDEs became systems of ODEs (describing the time-dependence of the Fourier amplitudes). The linear eigenmodes of the system were functions of  $\mathbf{k}$ . Thus, the expansion of the perturbations in terms of the eigenmodes took the following form:

$$\begin{pmatrix} u(\mathbf{k}, t) \\ p(\mathbf{k}, t) \\ \vdots \end{pmatrix} = \sum_{j=1}^N \beta_j(\mathbf{k}, t) \begin{pmatrix} u_j(\mathbf{k}) \\ p_j(\mathbf{k}) \\ \vdots \end{pmatrix}, \quad (7)$$

where  $N$  was the number of eigenmodes (also the number of dynamical fields considered),  $f_j(\mathbf{k}) = u_j(\mathbf{k}), p_j(\mathbf{k})$ ,

etc. are the components of the  $j$ th eigenvector, and  $\beta_j(\mathbf{k}, t)$  is the contribution of the  $j$ th eigenmode to the state of the system at  $(\mathbf{k}, t)$ , also called the eigenmode amplitude. The full nonlinear ODEs that describe the evolution of the perturbations were written in terms of the eigenmodes by substituting the dynamical quantities for the eigenmodes using Eq. (7). With some algebraic manipulations, the original nonlinear equations for  $\dot{u}, \dot{p}$ , etc. transform to equations for  $\dot{\beta}_j$ . These new ODEs are equivalent to the equations that govern the original dynamical system, but instead describe the nonlinear evolution of the system in terms of the eigenmode amplitudes. We refer to this process, both the expansion of the perturbations and the manipulation of their governing equations, as an eigenmode projection. The ODEs for the eigenmode amplitudes provide powerful insight into the system. The nonlinearities that couple the dynamical fields at different scales become nonlinearities that couple each of the eigenmodes at every scale. Thus, it was shown (and borne out by many simulations<sup>8</sup>) that despite decaying in the linear regime, the stable modes are driven by the unstable modes through the nonlinearity.

By comparing the magnitude of the nonlinearities that transfer energy to stable modes to the magnitude of the nonlinearities that cause the Kolmogorov-like cascade of energy from an unstable mode at one scale to the same mode at another scale, one can investigate how important stable modes are in instability saturation. A quantity known as the threshold parameter that evaluates the relative importance of the stable eigenmodes in instability saturation has been derived from the eigenmode-projected ODEs. If the threshold parameter is small compared to unity, it indicates that the instability saturates via a Kolmogorov-like transfer of energy to smaller scales, and only the term in Eq. (7) corresponding to the most unstable eigenmode need be included to accurately describe the system. If the threshold parameter is of order a few tenths or larger, it indicates the transfer of energy from the unstable mode to other modes at the same scale is an important mechanism in saturation. Additional terms in Eq. (7) must therefore be included.

In these previous calculations, the homogeneous nature of the system made the set of linear eigenmodes a complete basis: at every time  $t$  and wavevector  $\mathbf{k}$ , the linear modes could be used to expand the state of the system (i.e. Eq. (7)). Due to the inhomogeneity of the present system, the linear solutions aren't simply Fourier modes in  $z$ , so this system does not readily lend itself to the vector representation of Ref.<sup>8</sup>. Moreover, Eq. (1) admits only two eigenmodes which likely do not span arbitrary perturbations that satisfy the boundary conditions. So the true state of the system cannot be written exactly in the form of Eq. (7) with  $N = 2$ . In order to properly describe the evolution of the system given an arbitrary initial condition, the system could be expanded in appropriate orthogonal polynomials or investigated as an initial value problem with additional time-dependent basis functions that are linear solutions

of the problem. Previous work has demonstrated that for inviscid shear flows the initial value calculation leads to the “discrete” eigenmodes with time-dependence  $e^{int}$  described in the previous section, and an additional set of “continuum” modes<sup>15</sup>. These continuum modes either oscillate with frequency  $U_0/k$  or decay algebraically. For the present calculation we only consider perturbations that can be expressed as linear combinations of the two discrete eigenmodes  $\phi_1$  and  $\phi_2$ , representing a truncation of the complete system. If we are able to demonstrate a significant impact from  $\phi_2$ , that suffices to demonstrate the importance of stable modes, relative to existing models that only consider the unstable mode.

By focusing on perturbations that are linear combinations of  $\phi_1$  and  $\phi_2$ , the vector representation and invertible linear transformation between the state of the system and the eigenmode amplitudes of Ref.<sup>8</sup> can be recovered. Consequently, the governing equation, Eq. (1), can be manipulated to derive nonlinear equations that describe the evolution of the eigenmode amplitudes and their interactions. The method relies on the jump conditions given in Eq. (4). Since the jump conditions for one eigenmode differ from those for the other eigenmode, one can form an invertible map between the discontinuity of  $D\phi$  at each interface and the amplitude of each eigenmode. Additionally, because there are two jump conditions that will serve as our dynamical quantities, only the two eigenmodes of the previous section are needed to construct an invertible map between eigenmodes and dynamical quantities. To derive equations describing the nonlinear interaction between the eigenmodes, we start by deriving nonlinear jump conditions.

First, let  $\hat{\phi}(k, z, t) = \mathcal{F}[\Phi(x, z, t)]$  be the Fourier transformed (in  $x$ ) stream function, and assume

$$\hat{\phi}(k, z, t) = \beta_1(k, t)\phi_1(k, z) + \beta_2(k, t)\phi_2(k, z). \quad (8)$$

The nonlinear jump conditions are obtained by performing the same steps that led to Eq. (4) without dropping nonlinear terms (and explicitly taking the Fourier transform rather than assuming normal modes). Taking the Fourier transform and integrating from  $\pm d - \epsilon$  to  $\pm d + \epsilon$  with  $\epsilon \rightarrow 0$  yields

$$\begin{aligned} \frac{\partial}{\partial t} \hat{\Delta}_{\pm} \pm ikU_0 \hat{\Delta}_{\pm} \pm \frac{ikU_0}{d} \hat{\phi}(k, \pm d) \\ + \lim_{\epsilon \rightarrow 0} ik \int_{-\infty}^{\infty} \frac{dk'}{2\pi} [D\hat{\phi}(k', z)D\hat{\phi}(k'', z)] \Big|_{\pm d - \epsilon}^{\pm d + \epsilon} = 0, \end{aligned} \quad (9)$$

where  $k'' \equiv k - k'$ , and

$$\begin{aligned} \hat{\Delta}_{\pm}(k, t) &\equiv \lim_{\epsilon \rightarrow 0} D\hat{\phi}(k, \pm d + \epsilon, t) - D\hat{\phi}(k, \pm d - \epsilon, t) \\ &= \beta_1(k, t)\Delta_{\pm 1}(k) + \beta_2(k, t)\Delta_{\pm 2}(k), \end{aligned}$$

and

$$\Delta_{\pm j}(k) \equiv \lim_{\epsilon \rightarrow 0} D\phi_j(k, \pm d + \epsilon) - D\phi_j(k, \pm d - \epsilon)$$

are the discontinuities in  $D\hat{\phi}$  and  $D\phi_j$  at  $z = \pm d$ . With  $\hat{\phi}$  given by Eq. (8) and  $\phi_j$  given by Eq. (6), one can show

$$\phi_j(d) = \frac{-\Delta_{+j}}{2|k|} - \frac{\Delta_{-j}}{2|k|e^{2|k|d}}$$

and

$$\phi_j(-d) = \frac{-\Delta_{+j}}{2|k|e^{2|k|d}} - \frac{\Delta_{-j}}{2|k|}.$$

The  $\hat{\phi}(k, \pm d)$  term in Eq. (9) can then be written in terms of  $\hat{\Delta}_{\pm}$  to yield

$$\frac{\partial}{\partial t} \begin{pmatrix} \hat{\Delta}_+ \\ \hat{\Delta}_- \end{pmatrix} = \mathbf{D} \begin{pmatrix} \hat{\Delta}_+ \\ \hat{\Delta}_- \end{pmatrix} + \begin{pmatrix} N_+ \\ N_- \end{pmatrix}, \quad (10)$$

with

$$\mathbf{D} = ikU_0 \begin{pmatrix} \frac{1}{2|k|d} - 1 & \frac{e^{-2|k|d}}{2|k|d} \\ \frac{-e^{-2|k|d}}{2|k|d} & -\frac{1}{2|k|d} + 1 \end{pmatrix}, \quad (11)$$

and  $N_{\pm}$  representing the nonlinearities in Eq. (9). Note that taking  $N_{\pm} \rightarrow 0$  and  $\frac{\partial}{\partial t} \rightarrow in$  reduces this to the linear system solved in the previous section.

We now have all of the necessary tools to treat this system in a manner similar to the previously-mentioned calculations. Using our definitions for  $\hat{\Delta}_{\pm}$  and  $\Delta_{\pm j}$ , the  $z$ -derivative of Eq. (8) evaluated between  $z = \pm d + \epsilon$  and  $z = \pm d - \epsilon$  is

$$\begin{pmatrix} \hat{\Delta}_+ \\ \hat{\Delta}_- \end{pmatrix} = \mathbf{M} \begin{pmatrix} \beta_1 \\ \beta_2 \end{pmatrix}, \quad (12)$$

where

$$\mathbf{M} = \begin{pmatrix} \Delta_{+1} & \Delta_{+2} \\ \Delta_{-1} & \Delta_{-2} \end{pmatrix} = -2|k|e^{|k|d} \begin{pmatrix} 1 & 1 \\ b_1 & b_2 \end{pmatrix}. \quad (13)$$

Eq. (12) is equivalent to Eq. (7): for this calculation, the dynamical quantities that we use to specify the state of the system are  $\hat{\Delta}_{\pm}$ , and their eigenmode structure is given by the columns of the matrix  $\mathbf{M}$ . The governing nonlinear PDE, Eq. (1) has been rewritten as a system of nonlinear ODEs, Eq. (10). The linearized system of ODEs (Eq. (10) with  $N_{\pm} \rightarrow 0$ ) can be diagonalized: substituting  $\hat{\Delta}_{\pm}$  for  $\beta_j$  via Eq. (12) and multiplying by  $\mathbf{M}^{-1}$  on the left gives

$$\begin{pmatrix} \dot{\beta}_1 \\ \dot{\beta}_2 \end{pmatrix} = \mathbf{M}^{-1} \mathbf{D} \mathbf{M} \begin{pmatrix} \beta_1 \\ \beta_2 \end{pmatrix}, \quad (14)$$

where the matrix  $\mathbf{M}^{-1} \mathbf{D} \mathbf{M}$  is diagonal with entries  $i\omega_j$ .

The nonlinear interactions between the eigenmodes can now be investigated. Applying the steps that led to Eq. (14) to the full, nonlinear Eq. (10) yields

$$\begin{pmatrix} \dot{\beta}_1 \\ \dot{\beta}_2 \end{pmatrix} = \mathbf{M}^{-1} \mathbf{D} \mathbf{M} \begin{pmatrix} \beta_1 \\ \beta_2 \end{pmatrix} + \mathbf{M}^{-1} \begin{pmatrix} N_+ \\ N_- \end{pmatrix}, \quad (15)$$

where, again,  $N_{\pm}$  are the nonlinearities in Eq. (9). Using Eq. (8) and the forms for  $\phi_j$  given by Eq. (6),  $N_{\pm}$  can be written in terms of products of the form  $\beta_i \beta_j$  with  $i, j$  each taking values 1, 2. Eq. (15) then becomes

$$\begin{aligned} \dot{\beta}_1(k) = i\omega_1(k)\beta_1(k) &+ \int_{-\infty}^{\infty} \frac{dk'}{2\pi} [C_1(k, k')\beta_1(k')\beta_1(k'') \\ &+ C_2(k, k')\beta_1(k')\beta_2(k'') \\ &+ C_3(k, k')\beta_1(k'')\beta_2(k') + C_4(k, k')\beta_2(k')\beta_2(k'')], \end{aligned} \quad (16)$$

$$\begin{aligned} \dot{\beta}_2(k) = i\omega_2(k)\beta_2(k) &+ \int_{-\infty}^{\infty} \frac{dk'}{2\pi} [D_1(k, k')\beta_1(k')\beta_1(k'') \\ &+ D_2(k, k')\beta_1(k')\beta_2(k'') \\ &+ D_3(k, k')\beta_1(k'')\beta_2(k') + D_4(k, k')\beta_2(k')\beta_2(k'')]. \end{aligned} \quad (17)$$

The coefficients  $C_j, D_j$  arise from writing the nonlinearities  $N_{\pm}$  in the basis of the linear eigenmodes, so their functional forms include information about both the linear properties of the system and the nonlinearities  $N_{\pm}$ . Equations (16) and (17) are equivalent to Eq. (10), but they directly show how  $\beta_1$  and  $\beta_2$  interact. An analogy can be made here to the use of Elsässer variables in incompressible, homogeneous MHD turbulence. Written in terms of  $\mathbf{v}$  and  $\mathbf{B} = \mathbf{B}_0 + \mathbf{b}$ , the equations include nonlinear terms like  $\mathbf{v} \cdot \nabla \mathbf{b}$ . The linearized equations are solved by counterpropagating, noninteracting waves of the form  $\mathbf{z}^{\pm} = \mathbf{v} \pm \frac{\mathbf{b}}{\sqrt{4\pi\rho_0}}$ . By expressing the nonlinear equations in terms of  $\mathbf{z}^{\pm}$ , one finds that the only nonlinearity in the equation for  $\partial \mathbf{z}^{\pm} / \partial t$  is  $\mathbf{z}^{\mp} \cdot \nabla \mathbf{z}^{\pm}$ . Thus, it is the nonlinear interactions between these linearly noninteracting modes that drives the turbulence. In the present calculation, the linearly noninteracting  $\phi_1, \phi_2$  are comparable to  $\mathbf{z}^{\pm}$ , and the terms proportional to  $\beta_1(k')\beta_2(k'')$  and  $\beta_1(k'')\beta_2(k')$  are comparable to  $\mathbf{z}^{\mp} \cdot \nabla \mathbf{z}^{\pm}$ . However, unlike the  $\mathbf{z}^{\pm}$  equations, the  $\beta_j$  equations include other nonlinear terms that are proportional to  $\beta_j(k')\beta_j(k'')$ . If all of the nonlinearities are zero except for the  $C_1$  term, then the evolution of  $\beta_1(k)$  is just a combination of its linear drive  $i\omega_1(k)$  and three-wave interactions with  $\beta_1(k')$  and  $\beta_1(k-k')$ , allowing  $\phi_1$  to saturate through a Kolmogorov-like cascade to smaller scales. This is effectively what is assumed in standard quasilinear calculations of momentum transport, where only  $\phi_1, \omega_1$  are considered. Fig. 4 shows some of the nonlinear coupling coefficients plotted over a range of wavenumbers. Since  $D_1, C_2$ , and  $C_3$  are not identically zero, there is some interaction between the eigenmodes. Previous systems where such interactions have been demonstrated are all gyroradius-scale, quasihomogeneous systems driven by drift wave instabilities<sup>8,10</sup>. Eqs. (16) and (17) represent a demonstration that these interactions occur for larger-scale, inhomogeneous, neutral fluids.

Since the different energy transfer channels depend on different terms in Eqs. (16) and (17), the terms can be compared to assess the likelihood that the stable eigenmode plays a significant role in saturation. A quantity  $P_t$

has been defined to estimate the relative amplitudes of  $\beta_1$  and  $\beta_2$  in saturation<sup>8</sup>. The quantity  $P_t$  is a ratio of the nonlinear coupling coefficients and therefore also includes information about both linear and nonlinear properties of the system. In the following section, we numerically evaluate the nonlinear coupling coefficients to obtain the threshold parameter  $P_t$ .

#### IV. THE THRESHOLD PARAMETER

The threshold parameter is given in terms of quantities in Eqs.(16) and (17) by<sup>8,10</sup>

$$P_t = \frac{D_1(C_2 + C_3)}{C_1^2(2 - \omega_2/\omega_1)}. \quad (18)$$

The parameter is used as an order of magnitude estimate of the role that the nonlinearities coupling unstable modes to a stable mode play relative to the nonlinearities that couple unstable modes to each other. It was derived for systems governed by equations of the form Eqs. (16) and (17) where initial amplitudes of both modes are assumed to be infinitesimal. When the ratio  $D_1(C_2 + C_3)/C_1^2$  is small, stable modes are coupled to unstable ones strongly enough to impact the dynamics. When the ratio  $\omega_1/\omega_2$  is small, stable modes decay too quickly to reach amplitudes comparable to unstable modes. In both cases the threshold parameter is small. Previous work has shown that when  $P_t$  is at least a few tenths, stable modes are excited to levels comparable to unstable modes<sup>10</sup>.

Consider the evolution of the system from an infinitesimal amplitude near the peak in growth rate,  $kd \approx 0.4$ . When amplitudes are small, dynamics are linear, and  $\beta_2(k)$  decays as  $e^{i\omega_2(k)t}$  while each unstable mode grows exponentially. Eventually one of the  $D_1(k, k')\beta_1(k')\beta_1(k - k')$  terms becomes dominant in Eq. (17). Assuming  $D_1(k, k')$  does not vary strongly, the value of  $k'$  which produces the largest  $D_1(k, k')\beta_1(k')\beta_1(k - k')$  term is the value for which both  $k'$  and  $k - k'$  are near the peak in growth rate (however, note that three-mode interactions require three separate wavenumbers, so  $k$ ,  $k'$ , and  $k - k'$  must each be different values – this is consistent with the observation that each  $C_j, D_j$  in Fig. 4 is zero at  $k = k'$ ). Consider  $k'd = 0.45$  and  $(k - k')d = 0.35 \Rightarrow kd = 0.8$ . Then the growth of  $\beta_1(k')$  is given by Eq. (16). Considering only the terms relevant to this interaction, we have

$$\dot{\beta}_1(k') = i\omega_1(k')\beta_1(k') + \frac{1}{2\pi} [C_1(k', k' - k)\beta_1(k' - k)\beta_1(k) + C_2(k', k' - k)\beta_1(k' - k)\beta_2(k) + C_3(k', k)\beta_1(k' - k)\beta_2(k)].$$

Evaluating the threshold parameter using these arguments for each of the  $C_j$  and  $D_j$  gives  $P_t \approx 0.96$ , indicating that energy transfer to the  $\beta_2$  mode at  $kd = 0.8$  is as important to the saturation of the unstable mode

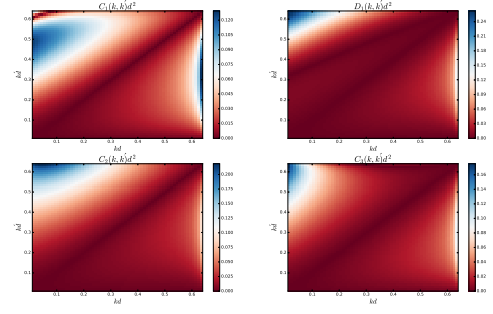


FIG. 4.  $C_1, C_2, C_3$ , and  $D_1$ , four of the nonlinear coupling coefficients in Eqs. (16) and (17), evaluated over the most relevant scales. The coefficients are in general complex. Here their absolute values are plotted.

at  $k'd = 0.35$  as the Kolmogorov-like transfer to unstable modes at other scales, and that  $\beta_2$  reaches saturation amplitudes comparable to  $\beta_1$ . The  $\beta_2$  mode at  $kd = 0.8$  is not linearly stable (all modes with  $|k|d \gtrsim 0.64$  are marginally stable), so this interaction does not directly lead to energy being transferred back into the equilibrium, but it is a mode that is ignored when one only considers the  $\beta_1$  modes. Going through the same steps with  $kd = 0.2, k'd = 0.55$  gives  $P_t \approx 0.88$ . So the linearly decaying mode at  $kd = 0.2$  plays an important role in saturation for the unstable mode at  $k'd = 0.55$ .

#### V. MOMENTUM TRANSPORT

We calculate the transport of momentum in the  $x$  direction across the interface at  $z = d$  in terms of the  $xz$ -component of the Reynolds stress tensor  $\tau_{xz} = \langle u_1 w_1 \rangle$  by integrating the  $x$ -component of the divergence of the tensor across the interface. Integrating  $D\tau_{xz}$  across the interface gives

$$S = -\lim_{\epsilon \rightarrow 0} \int_{d-\epsilon}^{d+\epsilon} dz \langle u_1 w_1 \rangle = -\lim_{\epsilon \rightarrow 0} \int_{d-\epsilon}^{d+\epsilon} dz D \langle D\Phi \frac{\partial \Phi}{\partial x} \rangle$$

where  $\langle \cdot \rangle$  denotes averaging in  $x$ ,  $u_1$  is the perturbed velocity in the  $x$  direction, and  $w_1$  is the perturbed velocity in the  $z$  direction. Taking  $\Phi = \mathcal{F}^{-1}[\hat{\phi}]$  with  $\hat{\phi} = \beta_1\phi_1 + \beta_2\phi_2$  gives

$$S = \int_{-\infty}^{\infty} \frac{dk}{2\pi} \frac{4k^2 d e^{2|k|d}}{U_0} [\text{Im}(\omega_1^*)|\beta_1|^2 + \text{Im}(\omega_2^*)|\beta_2|^2 + \text{Im}((\omega_2^* + kU_0)\beta_1\beta_2^*) + \text{Im}((\omega_1^* + kU_0)\beta_2\beta_1^*)]. \quad (19)$$

When the stable modes are ignored, only the first term contributes to  $S$ . The coefficient  $4k^2 d e^{2|k|d}/U_0$  is non-negative, and Eq. (5) shows that  $\text{Im}(\omega_1^*) \leq 0$  and  $\text{Im}(\omega_2^*) = -\text{Im}(\omega_1^*)$ , indicating that the transport due to stable modes alone is negative, and the second term acts against the first to reduce  $|S|$ . Clearly the amplitude

of  $\beta_2(k)$  relative to  $\beta_1(k)$  has a significant impact on the momentum transport in this system. The relative phase between  $\beta_2(k)$  and  $\beta_1(k)$  determines the contribution of the last two terms. If  $|\beta_2(k)| = |\beta_1(k)|$ , then the first two terms cancel and the transport is entirely determined by the last two terms. If the modes are in phase, then  $\beta_1\beta_2^*$  is real, and the last two terms cancel. Other systems exist where the last two terms dominate the relevant transport quantities<sup>7,9</sup>.

Ideally one would numerically solve Eqs. (16) and (17) for  $\beta_j(k)$  and integrate Eq. (19) to calculate  $S$ . In lieu of a numerical solution, we look for an order of magnitude approximation of the ratio  $|\beta_2(k)|^2/|\beta_1(k)|^2$  using the threshold parameter, and neglect the last two terms for an estimate of the contribution of  $\beta_2$  to the transport.

In the derivation of the threshold parameter, the interaction of an unstable mode at one wavenumber with a stable mode at another wavenumber is considered<sup>8</sup>. The growth of  $\beta_1$  is taken to be its linear growth, while  $\beta_2$  is shown to grow as

$$\beta_2 \approx \frac{D_1\beta_i^2}{\gamma_2 + 2\gamma_1} [e^{2\gamma_1 t} - e^{-\gamma_2 t} + \beta_i e^{-\gamma_2 t}],$$

where  $\beta_i$  is the initial amplitude of both modes (assumed small),  $\gamma_1 > 0$  is the growth rate of  $\beta_1$ , and  $\gamma_2 \geq 0$  is the decay rate of  $\beta_2$ . The saturation time is defined by  $\gamma_1 \approx C_1\beta_i e^{\gamma_1 t}$ , so the ratio  $\beta_2/\beta_1$  at the saturation time to leading order in  $\beta_i$  can be approximated as  $\beta_2/\beta_1 \approx \frac{D_1}{3C_1} = P_t \frac{C_1}{C_2+C_3} \approx P_t$ . Using the values of  $P_t$  from the previous section, we find that the stable modes reduce the momentum transport of the unstable modes by  $P_t^2 \approx 0.75 - 0.95$ .

## VI. CONCLUSION

We have presented an analysis of the unstable shear layer, an inhomogeneous system with global-scale, linearly stable and unstable modes where the stable modes are nonlinearly driven by the unstable modes. Previous demonstrations of the nonlinear excitation of linearly

stable modes and their impact on saturation and turbulence were limited to quasihomogeneous systems on length scales of the order of one gyroradius<sup>8,10</sup>. Whether stable mode excitation occurred in inhomogeneous systems and in systems with instability of global scales remained an open question.

Assuming the flow is a linear combination of the linear eigenmodes allows the global state of the system to be described in terms of its behavior at the edges of the layer. The nonlinearity, originally written in terms of flow components and their spatial derivatives, is then written in terms of the eigenmodes to demonstrate that it allows unstable modes to pump stable modes. This allows the eigenfunctions of this system to be treated similarly to the eigenvectors of previous systems. Using the threshold parameter, we have estimated the impact that stable modes have on instability saturation and found it to be significant. Finally, we consider the contribution that stable modes can have to momentum transport, and give an estimate in terms of the threshold parameter.

- <sup>1</sup>K.A. Browning, Quart. J. Roy. Met. Soc. **97**, pp. 283-299 (1971).
- <sup>2</sup>B.N. Rogers, W. Dorland, and M. Kotschenreuther, Phys. Rev. Lett. **85**, 5336-5339 (2000).
- <sup>3</sup>E.B. Churchwell, Astrophys. J. **479**, L59-L61 (1997).
- <sup>4</sup>K. Kwak, R.L. Shelton, and D.B. Henley, Astrophys. J. **812**, 111, 15 pp. (2015).
- <sup>5</sup>F.M. Rieger and P. Duffy, Astrophys. J. **652**, 1044-1049 (2006).
- <sup>6</sup>S. Chandrasekhar, *Hydrodynamic and Hydromagnetic Stability* (Oxford University Press, 1961).
- <sup>7</sup>D.A. Baver, P.W. Terry, R. Gatto, and E. Fernandez, Phys. Plasmas **9**, 3318 (2002).
- <sup>8</sup>P.W. Terry, D.A. Baver, and S. Gupta, Phys. Plasmas **13**, 022307 (2006).
- <sup>9</sup>P.W. Terry, D.A. Baver, and D.R. Hatch, Phys. Plasmas **16**, 122305 (2009).
- <sup>10</sup>K.D. Makwana, P.W. Terry, J.-H. Kim, and D.R. Hatch, Phys. Plasmas **18**, 012302 (2011).
- <sup>11</sup>D. Lecoanet, M. McCourt, E. Quataert, K.J. Burns, G.M. Vasil, J.S. Oishi, B.P. Brown, J.M. Stone, and R.M. O'Leary, Mon. Not. Roy. Ast. Soc. **455**, 4274 (2016).
- <sup>12</sup>M.L. Palotti, F. Heitsch, E.G. Zweibel, and Y.-M. Huang, Astrophys. J. **678**, 234-244 (2008).
- <sup>13</sup>P.W. Terry, and R. Gatto, Phys. Plasmas **13**, 062309 (2006).
- <sup>14</sup>M.J. Pueschel, B.J. Faber, J. Citrin, C.C. Hegna, P.W. Terry, and D.R. Hatch, Phys. Rev. Lett. **116**, 085001 (2016).
- <sup>15</sup>K.M. Case, Phys. Fluids **3**, 143 (1960).